Published in final edited form as:
J Hypertens. 2010 April ; 28(4): 806–816. doi:10.1097/HJH.0b013e3283358b6e.

Centrally administered lipopolysaccharide elicits sympathetic excitation via NAD(P)H oxidase-dependent mitogen-activated protein kinase signaling

Zhi-Hua Zhang[2], **Yang Yu**[2], **Shun-Guang Wei**[2], and **Robert B. Felder**[1,2]

[1]Medical Service, Department of Veterans Affairs Medical Center, Iowa City, IA

[2]Department of Internal Medicine, Roy J and Lucille A Carver College of Medicine, University of Iowa

Abstract

Objective—The mechanisms by which inflammation activates sympathetic drive in heart failure and hypertension remain ill-defined. In this study, an intracerebroventricular (ICV) injection of lipopolysaccharide (LPS) was used to induce the expression of cytokines and other inflammatory mediators in the brain, in the absence of other excitatory mediators, and the downstream signaling pathways leading to sympathetic activation were examined using ICV injections of blocking or inhibiting agents.

Methods and Results—In anesthetized rats, ICV injection of LPS (5 μg) increased ($p<0.05$) renal sympathetic nerve activity, blood pressure and heart rate. LPS increased ($p<0.05$) hypothalamic mRNA for NAD(P)H oxidase subunits p47 ^{phox} and gp91^{phox}, NAD(P)H-oxidase-dependent superoxide generation, hypothalamic mRNA for tumor necrosis factor (TNF)-α, cyclooxygenase-2 (COX-2), and cerebrospinal fluid (CSF) levels of TNF-α and prostaglandin E2 (PGE_2). In the paraventricular nucleus of hypothalamus, dihydroethidium staining for superoxide expression and c-Fos activity (indicating neuronal excitation) increased. The superoxide scavenger tempol significantly ($p<0.05$) diminished the expression of inflammatory mediators, as well as superoxide expression and neuronal excitation in paraventricular nucleus. SB203580 (p38 mitogen-activated protein kinase inhibitor) also reduced the expression of inflammatory mediators in hypothalamus and CSF. Tempol, apocynin (NAD(P)H oxidase inhibitor), SB203580 and NS398 (COX-2 inhibitor) all reduced CSF PGE_2 and the sympatho-excitatory response to LPS. LPS also increased angiotensin II type 1 receptor mRNA, a response blocked by apocynin and tempol but not by SB203580.

Conclusion—These findings suggest that central inflammation in pathophysiological conditions activates the sympathetic nervous system via NAD(P)H-oxidase and p38 mitogen-activated protein kinase dependent synthesis of PGE_2.

Corresponding Author: Robert B. Felder, MD, University of Iowa Carver College of Medicine, E318-GH, 200 Hawkins Drive, Iowa City, IA 52242, USA, Telephone: (319) 356-3642, FAX: (319) 353-6343, robert-felder@uiowa.edu.

DISCLOSURES

None

Keywords

lipopolysaccharide; inflammation; oxidative stress; prostaglandins; paraventricular nucleus of hypothalamus

INTRODUCTION

Lipopolysaccharide (LPS), or endotoxin, acts upon Toll-Like Receptor 4 to elicit an inflammatory response. An early and essential step in this process appears to be NAD(P)H oxidase-dependent production of reactive oxygen species (ROS), which in turn stimulate mitogen-activated protein kinase (MAPK) pathways [1–4]. While LPS activates all three of the major MAPK pathways [1], the p38 MAPK pathway seems most closely associated with LPS-induced upregulation of inflammatory mediators [5], including tumor necrosis factor – alpha (TNF-α), interleukin 1 – beta (IL-1β), and cyclooxygenase – 2 (COX-2), the inducible form of cyclooxygenase regulating synthesis of prostaglandin E2 (PGE_2). The impact of LPS-induced inflammation in the central nervous system may be dependent upon underlying conditions [6] and site of action [7].

In the present study, LPS was administered centrally to investigate the effect of inflammatory mediators in the brain on sympathetic regulation in normal rats. The study was predicated on our previous work demonstrating inflammation in cardiovascular regions of the brain in a rodent model of heart failure. In that model, ROS, TNF-α, IL-1β, and PGE_2 are all increased in the brain [8–11], but so are other neuroactive substances – i.e, angiotensin II [12] and aldosterone [13] - that may contribute to sympathetic excitation. Here we tested the hypothesis that the presence of these inflammatory mediators is sufficient to activate the sympathetic nervous system, independent of other factors. We also tested the hypothesis that inflammatory mediators upregulate the brain renin-angiotensin system, an alternative source of ROS and MAPK activity [14,15] and an important regulator of sympathetic activity. Our previous studies in rats with heart failure have suggested such an effect [9]. In this study, we focused on LPS-induced inflammatory changes in the hypothalamus and particularly the paraventricular nucleus (PVN) of the hypothalamus, a cardiovascular and autonomic center that has been implicated in the dysregulation of the sympathetic nervous system in heart failure [16–18].

METHODS

Experiments were performed on adult male Sprague-Dawley rats (300–350 g, Harlan Sprague Dawley, Indianapolis, IN). The animals were housed in the University of Iowa Animal Care Facility and exposed to a normal 12:12-h light-dark cycle. The studies were performed in accordance with the "Guiding Principles for Research Involving Animals and Human Beings" of the American Physiological Society [19]. The experimental procedures were approved by the Institutional Animal Care and Use Committee of the University of Iowa and the Research and Development Committee of the Iowa City Department of Veterans Affairs Medical Center.

General surgical preparation

Rats were anesthetized with urethane (1.5 g/kg, ip), and supplemental doses of urethane (0.1–0.3 g/kg, ip or iv) were given when increases in blood pressure (BP), heart rate (HR), or respiratory rate were observed during surgery or recording. The level of anesthesia was periodically reassessed during the surgical procedures and experimental recording by examining nociceptive reflex responses and by continuously monitoring BP and HR. The left femoral artery was cannulated with PE-50 tubing filled with heparinized saline (50 U/ml) connected to a pressure transducer for the recording of BP with a Hewlett-Packard 7754A chart recorder (HP Medical Products Group, Andover, MA). The left femoral vein was cannulated

with PE-20 tubing for the administration of drugs. Animals were intubated and breathed spontaneously. Core temperature was maintained at 37 ± 0.3°C with a temperature controller (model K-100, Baxter Healthcare, Valencia, CA). The head was fixed in a stereotaxic frame (David Kopf Instrument, Tujunga, CA). Stereotaxic coordinates for lateral cerebral ventricular injections were derived from the rat atlas of Paxinos and Watson [20].

Intracerebroventricular (ICV) injections

A 23-gauge stainless steel guide cannula was lowered into the left lateral cerebral ventricle using standard stereotaxic procedures. The coordinates with respect to bregma were -1.0 mm posterior, 1.5 mm lateral from the midline, and 3.5 mm ventral to dura. ICV bolus injections (LPS, NS398 and aCSF) were made in a volume of 2 μl over 10 seconds using a29-gauge stainless steel tubing. Other drugs (apocynin, tempol and SB203580) were administered by continuous ICV infusion at rate of 10μl/hr via a 29-gauge stainless steel cannula connected with PE-10 tubing to a Hamilton syringe driven by a Harvard Apparatus 11 pump (Model 55–1111, Holliston, MA) for 4-hour, starting at the time of the LPS injection. The ICV position of the cannula was confirmed by the staining of all four ventricles after injection of 2 μl pontamine sky blue at the end of the experiments in some rats.

Electrophysiological recording procedures

Recordings of renal sympathetic nerve activity (RSNA) were obtained from the left renal nerve using methods previously described from our lab [21–23]. In brief, the left kidney was exposed through a flank incision. A branch of the renal nerve was dissected free from surrounding tissue and placed on bipolar silver wire recording electrodes. When an optimal signal-to-noise ratio was established, the electrode and the renal nerve were covered with silicon sealant (World Precision Instruments, Sarasota, FL). The electrodes were sutured to the back muscles. The recording session began at least an hour after completion of the surgical preparation.

Renal nerve activity was amplified (model P511, Grass Instrument; Quincy, MA) and displayed on an oscilloscope (TDS 3014, Tektronix, Beaverton, OR). The noise level was finally determined at the end of experiment after ganglionic blockade with hexamethonium (30 mg/kg, iv). The net value of RSNA was calculated by subtracting the background noise from the actual recorded value during the experiment.

The BP signal and the rectified and integrated voltage from the renal nerve recording were fed into a data acquisition system consisting of a Cambridge Electronics Design (CED, Cambridge, UK) 1401 Plus computer interface coupled with a Dell Pentium personal computer. Mean blood pressure (MBP) and HR were derived from the arterial pressure tracing. MBP, HR and RSNA were averaged over a 3-minute interval every 30 minutes. A 3-min baseline was used as control. Because of the baseline variations from animal to animal, the data are presented as changes from baseline instead of absolute values. Windowed RSNA (spikes/sec) and integrated RSNA (mV) are shown in the figures, but the integrated RSNA was used for statistical analysis. Changes in integrated RSNA were calculated as a percent change from the baseline activity.

Hypothalamic tissue and cerebrospinal fluid (CSF) collections

To collect hypothalamic tissue and CSF for molecular studies, rats were deeply anesthetized with urethane (2.0 g/kg, ip). The hypothalamus was removed using the posterior part of the optic chiasm as the anterior limit, the anterior part of the mammillary bodies as the posterior limit, and the lateral hypothalamic sulci as the lateral limits, as described previously [8,23]. CSF was withdrawn from the cisterna magna and stored at − 80°C until assay.

Real-Time PCR

The total RNA was extracted from the brain hypothalamus using TRI Reagent (Molecular Research Center, Inc., Cincinnati, OH). Following reverse transcription of total RNA, quantification for mRNA expression of COX-2, TNF-α, NAD(P)H oxidase subunits (p47 ^{phox} and gp91^{phox}), angiotensin converting enzyme (ACE) and angiotensin II type 1 receptors (AT1R) were performed using a real-time PCR method described previously [10, 13,24]. The sequences for primers and probe used are summarized in Table 1. Primers and probes for GAPDH were purchased from Applied Biosystems (Foster City, CA). Real-time PCR was performed using the ABI prism 7000 Sequence Detection System (Applied Biosystems). The final results of real-time PCR were expressed as the ratio of mRNA of interest to GAPDH.

Western Blot

COX-2 and TNF-α protein levels were measured with a Western blotting technique as previously described [10,24,25], using polyclonal primary antibodies to COX-2 (Cayman Chemical Co, Ann Arbor, MI) and TNF-α (Santa Cruz Biotechnology Inc, Santa Cruz, CA). The density of the bands was quantified using National Institutes of Health Image-J analysis software.

Measurement of superoxide production

Superoxide production in the hypothalamus was measured using lucigenin-enhanced chemiluminescence [13,26,27]. Briefly, hypothalamic tissue was homogenized in cold Krebs/HEPES buffer (PH 7.4) for protein extraction. 30 μg protein was added to preheated Krebs/HEPES buffer (37°C) containing 5 μmol/L of lucigenin and then read in a Sirius luminometer at 30-s intervals for 10 minutes. The value was subtracted from background. NAD(P)H (100 μM) was used to stimulate NAD(P)H oxidase. To confirm the source of superoxide, samples were preincubated with diphenylene iodonium (DPI, 100 μM), a flavoprotein inhibitor of NAD(P)H oxidase. Chemiluminescence was reported as relative light units normalized to protein concentration.

Detection of c-Fos activity in PVN

Brain sections were processed for c-Fos activity using the avidin–biotin–peroxidase complex (ABC kit, PK-6101, Vector Laboratories, Inc., Burlingame, CA) technique, as previously described [13,23–25]. The sections were incubated for 24 hrs at 4°C with a rabbit anti-rat polyclonal anti-Fos antibody (K-25, 1:2000, Santa Cruz Biotechnology Inc., Santa Cruz, CA), followed by a secondary antibody (1:5000, biotinylated anti-rabbit IgG, PK-6101, Vector Laboratories, Inc.) for 1 hr at room temperature. The c-Fos positive neurons were colored with DAB kit (SK-4100, Vector Laboratories, Inc.). In each animal, c-Fos positive neurons within a standardized window superimposed over dorsal parvocellular (dpPVN), medial parvocellular (mpPVN), ventrolateral parvocellular (vlpPVN) and posterior magnocellular (pmPVN) subregions of PVN were counted manually, as previously described [13,23]. Counts from 2 representative 16-μm transverse sections approximately −1.80 mm from bregma were averaged to obtain a single value for data analysis. Data were represented as positive cells per 10^4 μm^2.

Detection of superoxide in PVN

Superoxide generation in the PVN was determined by fluorescent-labeled dihydroethidium (DHE; 2 μmol/L, Molecular Probes, Eugene, OR) staining for 30 minutes at 37°C in a light-protected humidified chamber, as previously described [13,26]. Images were visualized with laser confocal microscopy and analyzed with NIH Image-J software.

Measurement of CSF TNF-α and PGE_2

CSF levels of TNF-α and PGE_2 and plasma levels of TNF-α were measured using high-sensitivity ELISA kits (TNF-α, BioSource International Inc, Camarillo, CA; PGE_2, R&D Systems Inc, Minneapolis, MN).

Drugs administered

The NAD(P)H oxidase inhibitors apocynin and diphenyleneiodonium (DPI) chloride, hexamethonium bromide, lipopolysaccharide (LPS), the superoxide dismutase mimetic tempol, and the p38 MAPK inhibitor SB203580 were purchased from Sigma (St. Louis, MO). The specific COX-2 inhibitor NS398 was purchased from Cayman Chemical Co. (Ann Arbor, MI). Drugs were dissolved in artificial cerebrospinal fluid (aCSF) for intracerebroventricular (ICV) injection and in saline for intravenous injections. The doses of drugs used in the present study were derived from previous studies from our laboratory and others and were optimized in preliminary experiments.

Experimental protocols

1. LPS (5 μg in 2 μl) was injected as a bolus ICV to elicit an inflammatory response in the brain. In control experiments, aCSF (2 μl) was injected ICV.
2. To test the role of brain ROS in LPS-induced responses, either tempol (0.5 mg/10μl/hr) or apocynin (60 μg/10μl/hr) was administered as a 4-hour continuous ICV infusion started at the time of the LPS injection.
3. To test the role of p38 MAPK, SB203580 (5 μg/10μl/hr) was administered as a 4-hour continuous ICV infusion started at the time of the LPS injection.
4. To test the role of brain COX-2, NS398 (2μg in 2 μl) was administered as a single bolus ICV injection ~ 5 minutes prior to the LPS injection.

Three groups of rats were studied:

Group 1. These rats received an ICV injection of LPS (n=8) alone; aCSF alone (n=6); LPS followed immediately by a continuous 4 hour ICV infusion of tempol (n=5), apocynin (n=5), or SB203580 (n=6); or LPS preceded by a bolus ICV injection of NS398 (n=6). RSNA, BP and HR were recorded before and then for 4 hours after the LPS injection. As a control, the same dose of tempol, apocynin, SB203580 or NS 398 (n=4 for each group) was administrated ICV in rats that did not receive an ICV injection LPS. At the end of the recording sessions, the rats were euthanized to obtain CSF, trunk blood and brain tissues for molecular analysis.

Group 2. These rats received an ICV injection of LPS alone (n=7) or ICV LPS followed immediately by a 4 hour ICV infusion of tempol (n=6) or aCSF (n=6). Four hours after the LPS injection, rats were anesthetized and transcardially perfused with 4% paraformaldehyde in 0.1M PBS. Brains were removed and kept in the fixative for a further 24 h, then transferred to 30% sucrose in 0.1M PBS overnight. The fixed forebrain region containing PVN was sliced into 16 μm coronal sections with a cryostat. Sections were mounted on the slides and stored at −80°C for later immunohistochemical studies using c-Fos expression to assess neuronal excitation in PVN.

Group 3. These rats received an ICV injection of LPS alone (n=5) or ICV LPS followed immediately by a 4 hour ICV infusion of tempol (n=5) or aCSF (n=5). Four hours after the LPS injection, the rats were anesthetized and the brain was removed and immediately frozen at −80°C for 1 h. Frozen brain tissues were sliced into 30-μm coronal sections with a cryostat for dihydroethidium (DHE) staining to assess superoxide production.

Data acquisition and analysis

All values are expressed as means ± SE. Statistical significance among multiple comparisons was determined by two-way repeated-measures ANOVA followed by post hoc Tukey test. For other unpaired data, a Student's *t*-test was used for comparison between groups. $P < 0.05$ was considered to indicate statistical significance.

RESULTS

Cardiovascular and sympathetic responses to ICV LPS

ICV administration of LPS induced significant ($p<0.05$, versus baseline) increases of integrated RSNA (44.2 ± 7.2% from baseline), MBP (13.9 ± 2.5 mmHg from baseline of 98.3 ± 3.2 mmHg) and HR (97.2 ± 21.6 bpm from baseline of 317.2 ± 8.9 bpm) (Fig. 1 and Fig 5). These responses occurred 20~30 min after injection, peaked at approximately ~120 min, and lasted more than 240 min following injection. The same volume of aCSF (2 μl) administered ICV had no effects on RSNA, MBP or HR. There were no significant differences between groups in baseline values.

NAD(P)H oxidase dependent superoxide and sympathetic responses to LPS

The sympathetic responses to ICV LPS were significantly ($p<0.05$, versus LPS alone) diminished by continuous ICV infusion of the superoxide dismutase mimetic tempol (Fig. 1). Continuous infusion of the NAD(P)H oxidase inhibitor apocynin also significantly reduced the LPS-induced sympathetic responses, notably prolonging the onset latency of the responses (Fig. 1). Continuous ICV infusion of tempol or apocynin in rats that did not receive ICV LPS had no significant effects on RSNA, HR and MBP (data not shown). There were no significant differences between groups in baseline values. Because of its apparent greater effectiveness, in the dose chosen, tempol was used in subsequent studies of downstream molecular mechanisms. However, the effectiveness of higher doses of apocynin was not tested.

In hypothalamic tissues, ICV LPS significantly ($p<0.01$) increased mRNA for the NAD(P)H oxidase subunits p47 ^{phox} and gp91^{phox} (Fig. 2A and 2B). This upregulation of NAD(P)H oxidase subunits was associated with an increase in NAD(P)H oxidase-dependent superoxide generation, as indicated by near complete blockade of superoxide anion production by DPI (Fig. 2C).

In the PVN, intracellular superoxide production detected with DHE staining was abundant in all subregions in the LPS-treated rats, compared with aCSF-treated rats (Fig. 2D). ICV tempol significantly reduced the LPS-induced DHE fluorescence in both magnocellular and parvocellular regions of PVN (Fig. 2E). There was no difference across treatment groups in DHE staining in hypothalamic regions surrounding PVN (data not shown).

c-Fos expression, a marker of neuronal excitation, also increased significantly ($p<0.01$ versus aCSF) throughout the PVN (Fig. 3). Neurons in the dorsal pavocellular (dpPVN), medial parvocellular (mpPVN), ventrolateral pavocellular (vlpPVN), and posterior magnocellular (pmPVN) PVN were affected. Areas outside PVN, at the same stereotaxic level, had only scattered c-Fos expression, unaffected by ICV LPS. ICV tempol significantly reduced LPS-induced c-Fos expression in both magnocellular and parvocellular regions of PVN (Fig. 3).

Putative downstream neurochemical mediators of the sympathetic response to LPS

ICV LPS induced significant increases in TNF-α and COX-2 mRNA in the hypothalamus, as well as TNF-α and PGE_2 levels in CSF (Fig. 4). Scavenging superoxide with ICV tempol or blocking the p38 MAPK pathway with ICV SB203580 substantially reduced these responses. Inhibiting COX-2 activity with ICV NS398 prevented the LPS-induced increase in CSF

PGE_2, but not CSF TNF-α. ICV LPS had no effect on the plasma TNF-α level (data not shown). The cardiovascular and sympathetic responses to ICV LPS were markedly reduced by ICV SB203580, and completely abolished by the COX-2 inhibitor NS398 (Fig. 5). The same doses of SB203580 and NS398 had no significant effects on baseline RSNA, HR and MBP (data not shown), which did not differ among groups.

LPS and the brain RAS

ICV LPS increased hypothalamic AT1R mRNA expression, but not hypothalamic ACE mRNA expression (Fig. 6). ICV apocynin and ICV tempol prevented the LPS-induced increases in hypothalamic AT1R mRNA expression, but SB203580 had no apparent effect.

DISCUSSION

The present study demonstrates a prominent cardiovascular and sympathetic response to centrally administered LPS mediated entirely by inflammatory changes in the neurochemical milieu of the brain. ICV LPS increased the production of superoxide in the PVN of hypothalamus, hypothalamic synthesis of TNF-α and COX-2, and CSF TNF-α and PGE_2. LPS also induced increases in cardiovascular and sympathetic activity that were reduced by blocking central NAD(P)H oxidase activity or quenching superoxide, or by inhibiting p38 MAPK, and were entirely abolished by inhibiting COX-2 activity. ICV LPS stimulated the hypothalamic expression of AT1R mRNA, but not ACE mRNA, via an NAD(P)H oxidase-dependent pathway that does not require p38 MAPK. We conclude that ICV LPS stimulates the production of pro-inflammatory cytokines, resulting in NAD(P)H oxidase and p38 MAPK dependent synthesis of PGE_2, and that PGE_2 contributes to the LPS-induced sympatho-excitatory response. Moreover, inflammatory mediators upregulate the activity of at least one important component of the brain-renin angiotensin system, the AT1R, and may also influence sympathetic drive by that mechanism.

The effects of ICV LPS on inflammatory mediators closely resemble findings from *in vitro* studies examining the effects of LPS on microglia in culture. In that setting, LPS initiates a sequence of cellular signaling events that ultimately results in the synthesis of pro-inflammatory cytokines, COX-2 and PGE_2 [28–30]. Inhibition of NAD(P)H oxidase prevents LPS-induced activation of MAPK pathways [1], the nuclear transcription factor kappa B (NF-κB) [1] and subsequent downstream inflammatory events. Although all three major MAPK signaling pathways are activated by LPS, activation of the p38 MAPK pathway appears to be necessary for the production of inflammatory mediators [30–32]. Inhibition of p38 MAPK reduces NF-κB dependent gene expression [32] and the generation of pro-inflammatory cytokines [32] and COX-2 [30].

Infectious and ischemic processes in the central nervous system stimulate microglia to produce large quantities of inflammatory mediators, including TNF-α, IL-1β, IL-6, NAD(P)H oxidase-dependent superoxide, and COX-2 [28–30]. We have observed a similar profile of inflammatory mediators in cardiovascular regulatory regions of the brain in rats with ischemia-induced heart failure [8,9,25]. Microglia are activated in this model of heart failure [33], though the mechanism is not known and the intensity of the inflammatory response may differ from that observed in infections and ischemic conditions. LPS is present in the circulation in heart failure - with gut as a primary source [34] – but is unlikely to cross the blood-brain barrier [35,36]. However, LPS induces the peripheral synthesis and release of pro-inflammatory cytokines, and it has been suggested that these cytokines may activate the microglia via their effects on cells of the blood brain barrier [35]. Thus, the presence of pro-inflammatory cytokines in brain tissue of rats with heart failure [9] may be either a cause or an effect, or both, of microglial activation. Unpublished data from our laboratory, using minocycline to inhibit

microglial activation [37], suggest that at least some of the inflammatory mediators present in the heart failure brain are a result of microglial activation.

This study in normal rats has demonstrated that inflammatory mediators in the brain can augment sympathetic nerve activity in normal rats independent of other influential factors that are present in the brain in heart failure. Principal among those other influential factors is angiotensin II, which also activates NAD(P)H oxidase-dependent superoxide production[38] and MAPK signaling pathways [39–42]. NAD(P)H oxidase-dependent superoxide generation in the brain leads to an increase in sympathetic nerve activity [38,43] that can be reduced by blocking either NAD(P)H oxidase activity [38] or by quenching ROS [38,44]. Angiotensin II-induced NAD(P)H oxidase-dependent superoxide production upregulates AT1R receptors [14,45], which may contribute to the increased sympathetic drive. In this study, LPS-induced NAD(P)H oxidase activity and increased expression of AT1R mRNA, suggesting that angiotensin II and the pro-inflammatory cytokines may share a common mechanism for upregulating AT1R. However, the downstream effects of these two ROS generating systems may be differentially regulated. In the present study, the p38 inhibitor had no effect on LPS induced AT1R activity, but substantially reduced mRNA for TNF-α and COX-2. We did not test the effect of inhibiting other MAPK pathways. “Compartmentalization” has been invoked to explain the commonly observed finding that different agents capable of activating the same MAPK pathways may produce different outcomes [46].

In summary, as illustrated by the schematic (Fig. 7), our data suggest that brain pro-inflammatory cytokines activate NAD(P)H oxidase dependent superoxide production and redox sensitive p38 MAPK activity [1–4], ultimately (via gene transcription) resulting in the generation of COX-2 and PGE_2, which is known to activate the sympathetic nervous system [21,47,48]. Agents that block or inhibit this putative pathway effectively reduce LPS-induced sympathetic drive. However, only those agents that block (apocynin) or scavenge (tempol) superoxide prevent the LPS-induced expression of AT1R.

Finally, the potential toxic effects of ICV LPS deserve comment. Central administration of LPS *in vivo* can induce neuronal injury [7] and impaired neurogenesis in response to neuronal injury [49], presumably caused by excessive release of inflammatory mediators by activated microglia. LPS induced injury appears to be greatest in areas with the greatest density of microglia [7]; in that study, microinjection of LPS (5 μg in 2 μl) directly into brain tissue caused loss of dopaminergic and other neurons in substantia nigra, which has the highest density of microglia, but no loss of neurons in hippocampus and cortex [7]. However, ICV doses in this same range and higher have been used successfully in studies examining physiological responses [50,51].

Perspectives

Inflammation is increasingly recognized to play an important role in cardiovascular diseases, including hypertension [52] and heart failure [9,10,24,53]. Recent studies have suggested a previously unrecognized role for inflammatory mediators in the brain in the regulation of the sympathetic nervous system in these conditions. The results of the present study suggest that NAD(P)H oxidase-dependent superoxide production and the redox sensitive p38 MAPK activity in the hypothalamus and PVN contribute to the sympatho-excitatory effects of the pro-inflammatory cytokines. The recent demonstration that brain MAPK signaling is an important factor sustaining sympathetic drive in heart failure [41] is consistent with that suggestion. Similar inflammation-induced molecular events may occur in other autonomic/presympathetic regions of the brain not studied here, e.g., the rostral ventrolateral medulla. These molecular mechanisms may be a substrate for the “cross-talk”

that has been described [11,54] between the cytokines and the brain renin-angiotensin system, as illustrated here by the LPS-induced upregulation of AT1R expression.

Acknowledgments

None

GRANTS

This material is based upon work supported in part by the Department of Veterans Affairs, Veterans Health Administration, Office of Research and Development, Biomedical Laboratory Research and Development, by NIH RO1 HL-073986 (to RBF) and by institutional funds provided by the University of Iowa

REFERENCES

1. Pawate S, Shen Q, Fan F, Bhat NR. Redox regulation of glial inflammatory response to lipopolysaccharide and interferongamma. J Neurosci Res 2004;77:540–551. [PubMed: 15264224]
2. Qin L, Liu Y, Wang T, Wei SJ, Block ML, Wilson B, Liu B, Hong JS. NADPH oxidase mediates lipopolysaccharide-induced neurotoxicity and proinflammatory gene expression in activated microglia. J Biol Chem 2004;279:1415–1421. [PubMed: 14578353]
3. Block ML, Hong JS. Microglia and inflammation-mediated neurodegeneration: multiple triggers with a common mechanism. Prog Neurobiol 2005;76:77–98. [PubMed: 16081203]
4. Qin L, Li G, Qian X, Liu Y, Wu X, Liu B, Hong JS, Block ML. Interactive role of the toll-like receptor 4 and reactive oxygen species in LPS-induced microglia activation. Glia 2005;52:78–84. [PubMed: 15920727]
5. Krishna M, Narang H. The complexity of mitogen-activated protein kinases (MAPKs) made simple. Cell Mol Life Sci 2008;65:3525–3544. [PubMed: 18668205]
6. Hanisch UK, Johnson TV, Kipnis J. Toll-like receptors: roles in neuroprotection? Trends Neurosci 2008;31:176–182. [PubMed: 18329736]
7. Kim WG, Mohney RP, Wilson B, Jeohn GH, Liu B, Hong JS. Regional difference in susceptibility to lipopolysaccharide-induced neurotoxicity in the rat brain: role of microglia. J Neurosci 2000;20:6309–6316. [PubMed: 10934283]
8. Francis J, Chu Y, Johnson AK, Weiss RM, Felder RB. Acute myocardial infarction induces hypothalamic cytokine synthesis. Am J Physiol Heart Circ Physiol 2004;286:H2264–H2271. [PubMed: 15148057]
9. Kang YM, Zhang ZH, Xue B, Weiss RM, Felder RB. Inhibition of brain proinflammatory cytokine synthesis reduces hypothalamic excitation in rats with ischemia-induced heart failure. Am J Physiol Heart Circ Physiol 2008;295:H227–H236. [PubMed: 18487441]
10. Yu Y, Zhang ZH, Wei SG, Chu Y, Weiss RM, Heistad DD, Felder RB. Central gene transfer of interleukin-10 reduces hypothalamic inflammation and evidence of heart failure in rats after myocardial infarction. Circ Res 2007;101:304–312. [PubMed: 17569888]
11. Guggilam A, Patel KP, Haque M, Ebenezer PJ, Kapusta DR, Francis J. Cytokine blockade attenuates sympathoexcitation in heart failure: cross-talk between nNOS, AT-1R and cytokines in the hypothalamic paraventricular nucleus. Eur J Heart Fail 2008;10:625–634. [PubMed: 18550427]
12. Zhang W, Huang BS, Leenen FH. Brain renin-angiotensin system and sympathetic hyperactivity in rats after myocardial infarction. Am J Physiol 1999;276:H1608–H1615. [PubMed: 10330245]
13. Yu Y, Wei SG, Zhang ZH, Gomez-Sanchez E, Weiss RM, Felder RB. Does aldosterone upregulate the brain renin-angiotensin system in rats with heart failure? Hypertension 2008;51:727–733. [PubMed: 18227408]
14. Zucker IH. Novel mechanisms of sympathetic regulation in chronic heart failure. Hypertension 2006;48:1005–1011. [PubMed: 17015773]
15. Infanger DW, Sharma RV, Davisson RL. NADPH oxidases of the brain: distribution, regulation, and function. Antioxid Redox Signal 2006;8:1583–1596. [PubMed: 16987013]

16. Patel KP. Role of paraventricular nucleus in mediating sympathetic outflow in heart failure. Heart Fail Rev 2000;5:73–86. [PubMed: 16228917]
17. Felder RB, Francis J, Zhang ZH, Wei SG, Weiss RM, Johnson AK. Heart failure and the brain: new perspectives. Am J Physiol Regul Integr Comp Physiol 2003;284:R259–R276. [PubMed: 12529279]
18. Felder RB, Francis J, Weiss RM, Zhang ZH, Wei SG, Johnson AK. Neurohumoral regulation in ischemia-induced heart failure. Role of the forebrain. Ann N Y Acad Sci 2001;940:444–453. [PubMed: 11458700]
19. American Physiological Society. Guiding principles for research involving animals and human beings. Am J Physiol Regul Integr Comp Physiol 2002;283:R281–R283. [PubMed: 12121837]
20. Paxinos, G.; Watson, C. The rat brain is stereotaxic coordinates. Sydney: Academic Press; 1986.
21. Zhang ZH, Wei SG, Francis J, Felder RB. Cardiovascular and renal sympathetic activation by blood-borne TNF-alpha in rat: the role of central prostaglandins. Am J Physiol Regul Integr Comp Physiol 2003;284:R916–R927. [PubMed: 12626358]
22. Wei SG, Felder RB. Forebrain renin-angiotensin system has a tonic excitatory influence on renal sympathetic nerve activity. Am J Physiol Heart Circ Physiol 2002;282:H890–H895. [PubMed: 11834483]
23. Zhang ZH, Yu Y, Kang YM, Wei SG, Felder RB. Aldosterone acts centrally to increase brain renin-angiotensin system activity and oxidative stress in normal rats. Am J Physiol Heart Circ Physiol 2008;294:H1067–H1074. [PubMed: 18162560]
24. Yu Y, Kang YM, Zhang ZH, Wei SG, Chu Y, Weiss RM, Felder RB. Increased cyclooxygenase-2 expression in hypothalamic paraventricular nucleus in rats with heart failure: role of nuclear factor kappaB. Hypertension 2007;49:511–518. [PubMed: 17242297]
25. Kang YM, Zhang ZH, Johnson RF, Yu Y, Beltz T, Johnson AK, Weiss RM, Felder RB. Novel effect of mineralocorticoid receptor antagonism to reduce proinflammatory cytokines and hypothalamic activation in rats with ischemia-induced heart failure. Circ Res 2006;99:758–766. [PubMed: 16960100]
26. Pan YX, Gao L, Wang WZ, Zheng H, Liu D, Patel KP, Zucker IH, Wang W. Exercise training prevents arterial baroreflex dysfunction in rats treated with central angiotensin II. Hypertension 2007;49:519–527. [PubMed: 17224469]
27. Ma X, Zhang HJ, Whiteis CA, Tian X, Davisson RL, Kregel KC, Abboud FM, Chapleau MW. NAD(P)H oxidase-induced oxidative stress in sympathetic ganglia of apolipoprotein E deficient mice. Auton Neurosci 2006;126–127:285–291.
28. Qin L, Block ML, Liu Y, Bienstock RJ, Pei Z, Zhang W, Wu X, Wilson B, Burka T, Hong JS. Microglial NADPH oxidase is a novel target for femtomolar neuroprotection against oxidative stress. Faseb J 2005;19:550–557. [PubMed: 15791005]
29. Wang T, Qin L, Liu B, Liu Y, Wilson B, Eling TE, Langenbach R, Taniura S, Hong JS. Role of reactive oxygen species in LPS-induced production of prostaglandin E2 in microglia. J Neurochem 2004;88:939–947. [PubMed: 14756815]
30. Akundi RS, Candelario-Jalil E, Hess S, Hull M, Lieb K, Gebicke-Haerter PJ, Fiebich BL. Signal transduction pathways regulating cyclooxygenase-2 in lipopolysaccharide-activated primary rat microglia. Glia 2005;51:199–208. [PubMed: 15800925]
31. Uesugi M, Nakajima K, Tohyama Y, Kohsaka S, Kurihara T. Nonparticipation of nuclear factor kappa B (NFkappaB) in the signaling cascade of c-Jun N-terminal kinase (JNK)-and p38 mitogen-activated protein kinase (p38MAPK)-dependent tumor necrosis factor 26 alpha (TNFalpha) induction in lipopolysaccharide (LPS)-stimulated microglia. Brain Res 2006;1073–1074:48–59.
32. Kaminska B. MAPK signalling pathways as molecular targets for anti-inflammatory therapy--from molecular mechanisms to therapeutic benefits. Biochim Biophys Acta 2005;1754:253–262. [PubMed: 16198162]
33. Kang YM, Shao JQ, Zhang ZH, Weiss RM, Johnson AK, Felder RB. Activation of microglia in paraventricular nucleus of hypothalamus: A source of central cytokine release in heart failure. Circulation 2005;112 II 192 (abstract).
34. Charalambous BM, Stephens RC, Feavers IM, Montgomery HE. Role of bacterial endotoxin in chronic heart failure: the gut of the matter. Shock 2007;28:15–23. [PubMed: 17510602]

35. Buttini M, Limonta S, Boddeke HW. Peripheral administration of lipopolysaccharide induces activation of microglial cells in rat brain. Neurochem Int 1996;29:25–35. [PubMed: 8808786]
36. Singh AK, Jiang Y. How does peripheral lipopolysaccharide induce gene expression in the brain of rats? Toxicology 2004;201:197–207. [PubMed: 15297033]
37. Tikka T, Fiebich BL, Goldsteins G, Keinanen R, Koistinaho J. Minocycline, a tetracycline derivative, is neuroprotective against excitotoxicity by inhibiting activation and proliferation of microglia. J Neurosci 2001;21:2580–2588. [PubMed: 11306611]
38. Gao L, Wang W, Li YL, Schultz HD, Liu D, Cornish KG, Zucker IH. Superoxide mediates sympathoexcitation in heart failure: roles of angiotensin II and NAD(P)H oxidase. Circ Res 2004;95:937–944. [PubMed: 15459075]
39. Zucker IH, Gao L. The regulation of sympathetic nerve activity by angiotensin II involves reactive oxygen species and MAPK. Circ Res 2005;97:737–739. [PubMed: 16224073]
40. Chan SH, Hsu KS, Huang CC, Wang LL, Ou CC, Chan JY. NADPH oxidase-derived superoxide anion mediates angiotensin II-induced pressor effect via activation of p38 mitogen-activated protein kinase in the rostral ventrolateral medulla. Circ Res 2005;97:772–780. [PubMed: 16151022]
41. Wei SG, Yu Y, Zhang ZH, Weiss RM, Felder RB. Mitogen-activated protein kinases mediate upregulation of hypothalamic angiotensin II type 1 receptors in heart failure rats. Hypertension 2008;52:679–686. [PubMed: 18768402]
42. Wei SG, Yu Y, Zhang ZH, Weiss RM, Felder RB. Angiotensin II-triggered p44/42 mitogen-activated protein kinase mediates sympathetic excitation in heart failure rats. Hypertension 2008;52:342–350. [PubMed: 18574076]
43. Zimmerman MC, Lazartigues E, Lang JA, Sinnayah P, Ahmad IM, Spitz DR, Davisson RL. Superoxide mediates the actions of angiotensin II in the central nervous system. Circ Res 2002;91:1038–1045. [PubMed: 12456490]
44. Lindley TE, Doobay MF, Sharma RV, Davisson RL. Superoxide is involved in the central nervous system activation and sympathoexcitation of myocardial infarction-induced heart failure. Circ Res 2004;94:402–409. [PubMed: 14684626]
45. Gao L, Wang W, Li YL, Schultz HD, Liu D, Cornish KG, Zucker IH. Sympathoexcitation by central ANG II: roles for AT1 receptor upregulation and NAD(P)H oxidase in RVLM. Am J Physiol Heart Circ Physiol 2005;288:H2271–H2279. [PubMed: 15637113]
46. Brown MD, Sacks DB. Compartmentalised MAPK pathways. Handb Exp Pharmacol 2008:205–235. [PubMed: 18491054]
47. Felder RB. Mineralocorticoid receptors, inflammation and sympathetic drive in heart failure. Exp Physiol 2010;95:19–25. [PubMed: 19648480]
48. Felder RB, Yu Y, Zhang ZH, Wei SG. Pharmacological treatment for heart failure: a view from the brain. Clin Pharmacol Ther 2009;86:216–220. [PubMed: 19553933]
49. Ekdahl CT, Claasen JH, Bonde S, Kokaia Z, Lindvall O. Inflammation is detrimental for neurogenesis in adult brain. Proc Natl Acad Sci U S A 2003;100:13632–13637. [PubMed: 14581618]
50. Ebisui O, Fukata J, Tominaga T, Murakami N, Kobayashi H, Segawa H, Muro S, Naito Y, Nakai Y, Masui Y, et al. Roles of interleukin-1 alpha and -1 beta in endotoxin-induced suppression of plasma gonadotropin levels in rats. Endocrinology 1992;130:3307–3313. [PubMed: 1597143]
51. Foca A, Altavilla D, Mondello F, Nicoletta P, Miragliotta G, Mastroeni P, Caputi AP. Cardiovascular responses of conscious rats to acute intravenous and intracerebroventricular administration of Shigella sonnei endotoxin. Res Commun Chem Pathol Pharmacol 1983;42:213–222. [PubMed: 6361936]
52. Granger JP. An emerging role for inflammatory cytokines in hypertension. Am J Physiol Heart Circ Physiol 2006;290:H923–H924. [PubMed: 16467462]
53. Kang YM, He RL, Yang LM, Qin DN, Guggilam A, Elks C, Yan N, Guo Z, Francis J. Brain tumour necrosis factor-alpha modulates neurotransmitters in hypothalamic paraventricular nucleus in heart failure. Cardiovasc Res 2009;83:737–746. [PubMed: 19457890]
54. Kang YM, Ma Y, Elks C, Zheng JP, Yang ZM, Francis J. Cross-talk between cytokines and renin-angiotensin in hypothalamic paraventricular nucleus in heart failure: role of nuclear factor-kappaB. Cardiovasc Res 2008;79:671–678. [PubMed: 18469338]

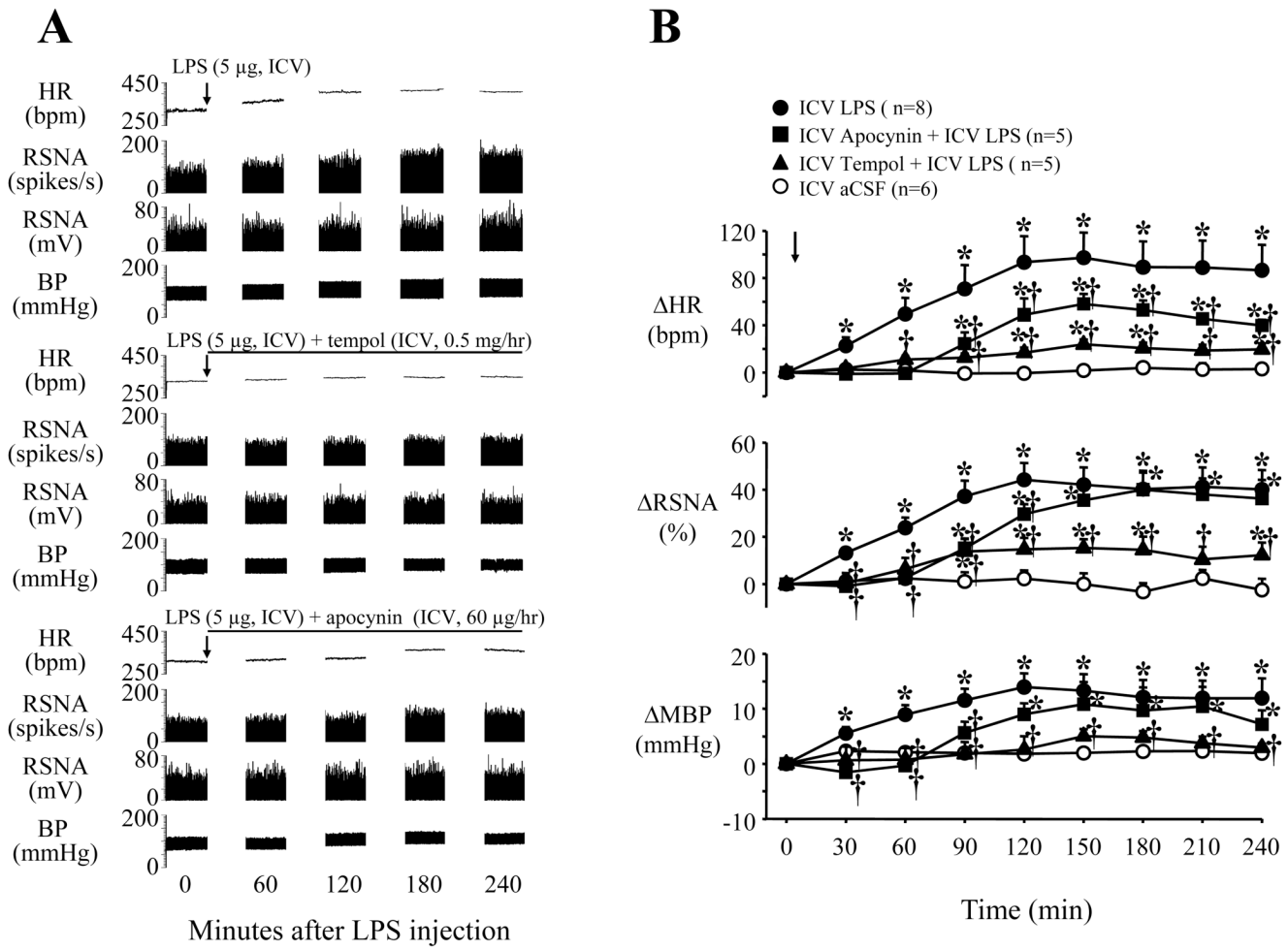

Fig. 1.

Representative recordings (**A**) and grouped data (**B**) showing LPS-induced increases in heart rate (HR), renal sympathetic nerve activity (RSNA) and blood pressure (BP) or mean BP (MBP) were prevented by continuous intracerebroventricular (ICV) infusion of tempol and diminished by apocynin infusion. Arrows indicate the LPS injection. Lines represent the continuous ICV infusion of tempol or apocynin. Each recording section is 200 seconds in duration with interval of 60 min. Values were expressed as mean ± SE. **P*<0.05, versus baseline, †*P*<0.05 versus ICV LPS alone.

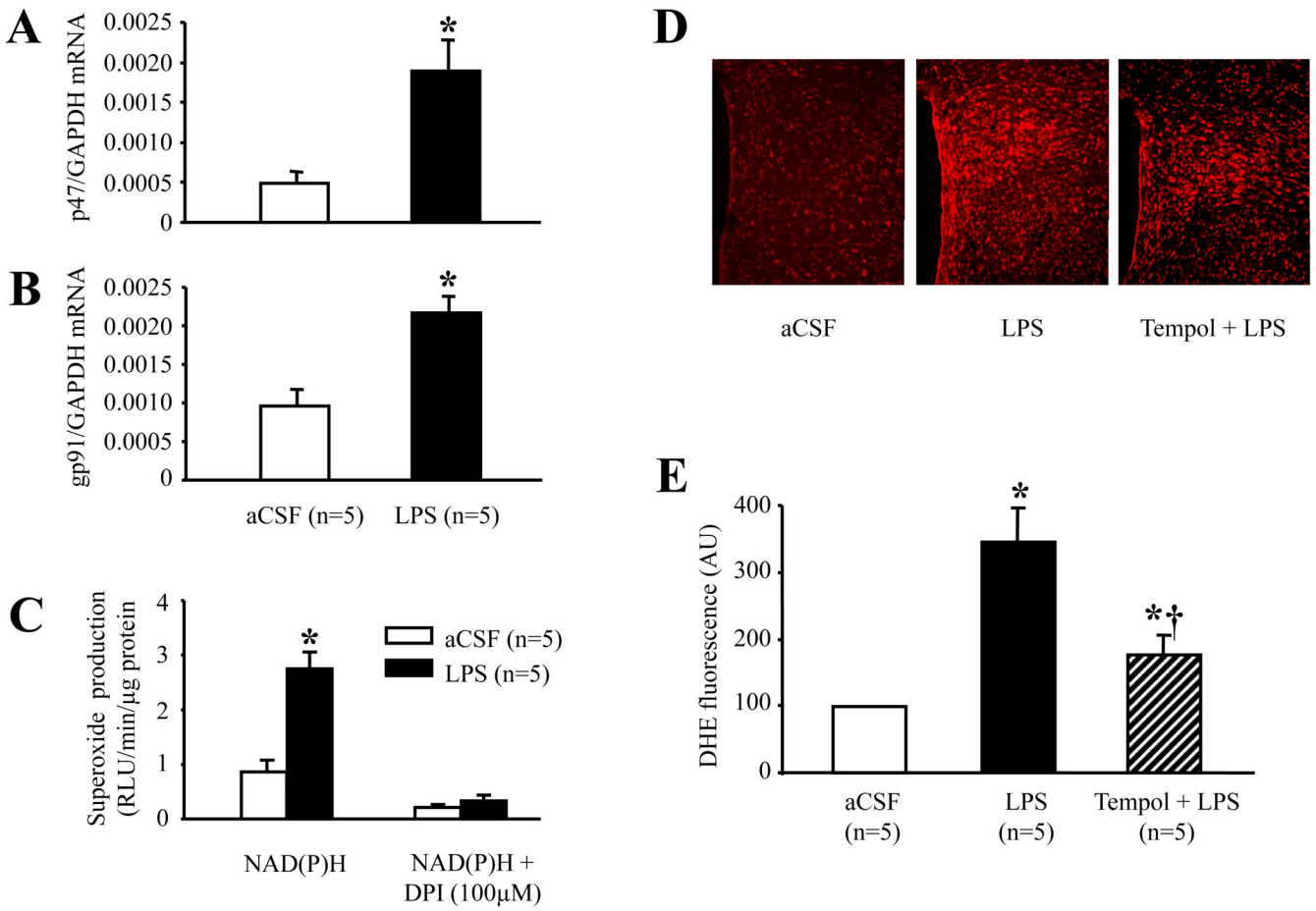

Fig. 2.

Quantitative mRNA expression of representative subunits of NAD(P)H oxidase $p47^{phox}$ (**A**) and $gp91^{phox}$ (**B**), and superoxide production (**C**) in the hypothalamus of rats treated with ICV aCSF or ICV LPS. **D:** Representative confocal images of PVN sections showing that dihydroethidium (DHE) fluorescence was abundant in the PVN of ICV LPS-treated rats compared with ICV aCSF-treated rats. Rats treated with ICV tempol in addition to LPS had less DHE fluorescence in the PVN than rats treated with ICV LPS alone. **E:** Quantitative comparison of DHE immunofluorescence in the PVN for each group. Values were expressed as mean ± SE. **P*<0.05 versus ICV aCSF, †*P*<0.05, ICV Tempol + ICV LPS versus ICV LPS alone.

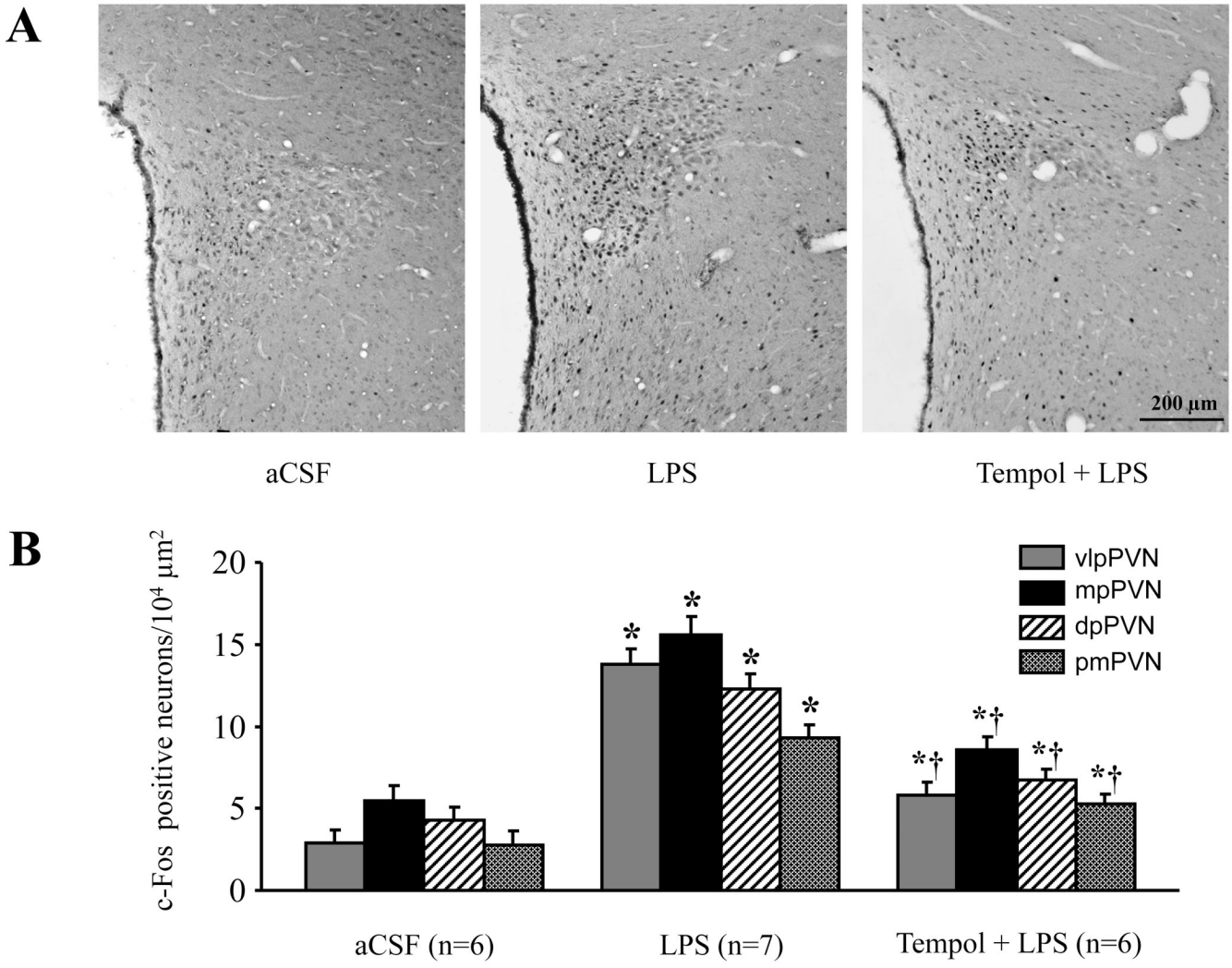

Fig. 3.

Expression of c-Fos activity in the PVN of hypothalamus. **A:** Representative sections showing ICV LPS treatment increased c-Fos immunoreactivity in the PVN neurons. ICV tempol treatment reduced LPS-induced c-Fos immunoreactivity in the PVN region. Dark dots indicate individual activated neurons. **B:** Quantification of c-Fos positive neurons in the dorsal pavocellular (dpPVN), medial parvocellular (mpPVN), ventrolateral pavocellular (vlpPVN), and posterior magnocellular (pmPVN) PVN. Values were expressed as mean ± SE. **P*<0.05 versus ICV aCSF, †*P*<0.05, ICV Tempol + ICV LPS versus ICV LPS alone.

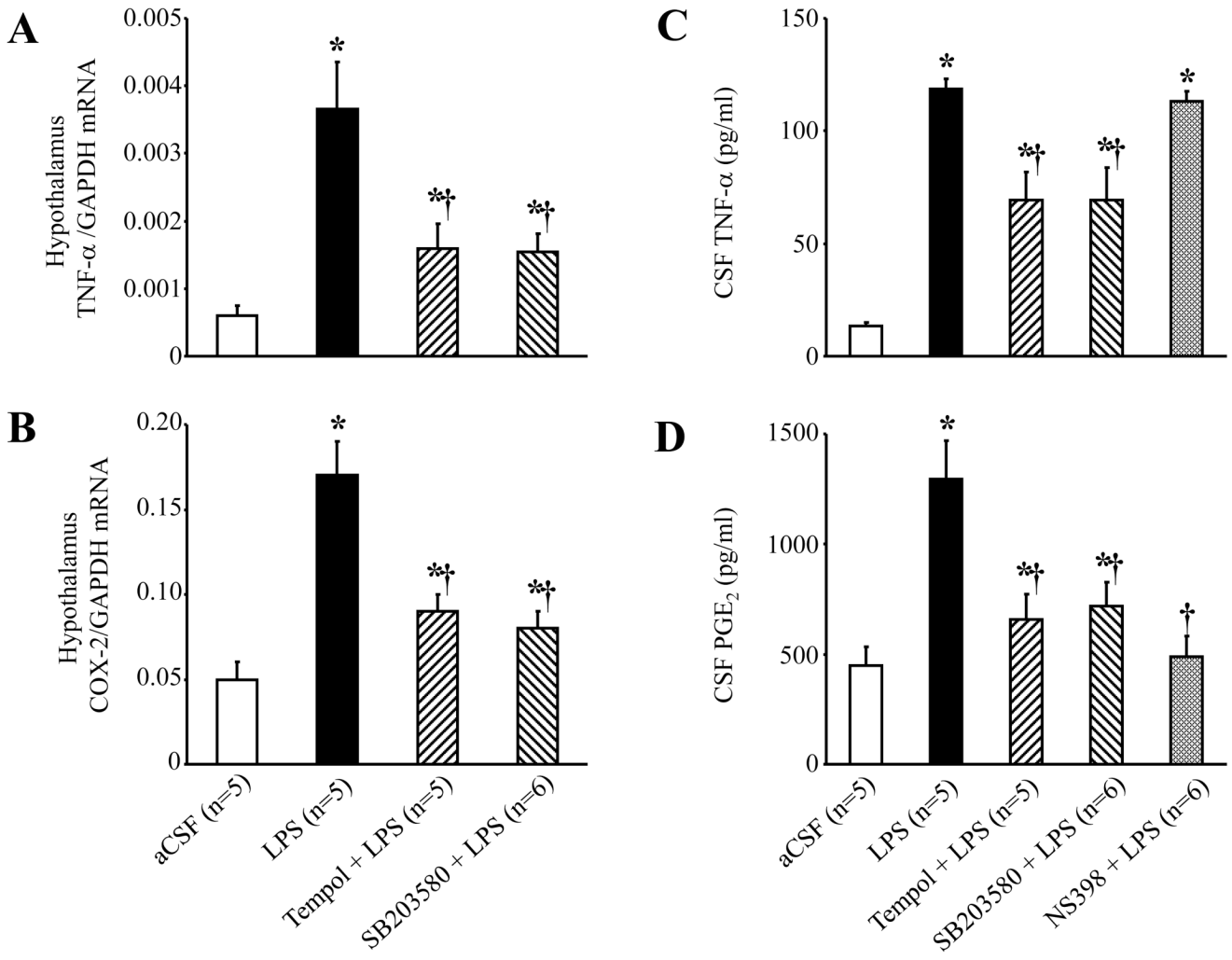

Fig. 4.

ICV administration of LPS increased hypothalamic tissue TNF-α (**A**) and COX-2 (**B**) mRNA expression, and both were significantly reduced by continuous ICV infusion of tempol and SB203580. ICV LPS also significantly increased cerebrospinal fluid (CSF) level of TNF-α (**C**) and PGE_2 (**D**). ICV infusion of tempol and SB203580 reduced the LPS-induced increases in CSF TNF-α and PGE_2; the COX-2 inhibitor NS398 reduced the LPS-induced increase in CSF PGE_2. **P*<0.05 versus ICV aCSF, †*P*<0.05, ICV Treatment + ICV LPS versus ICV LPS alone.

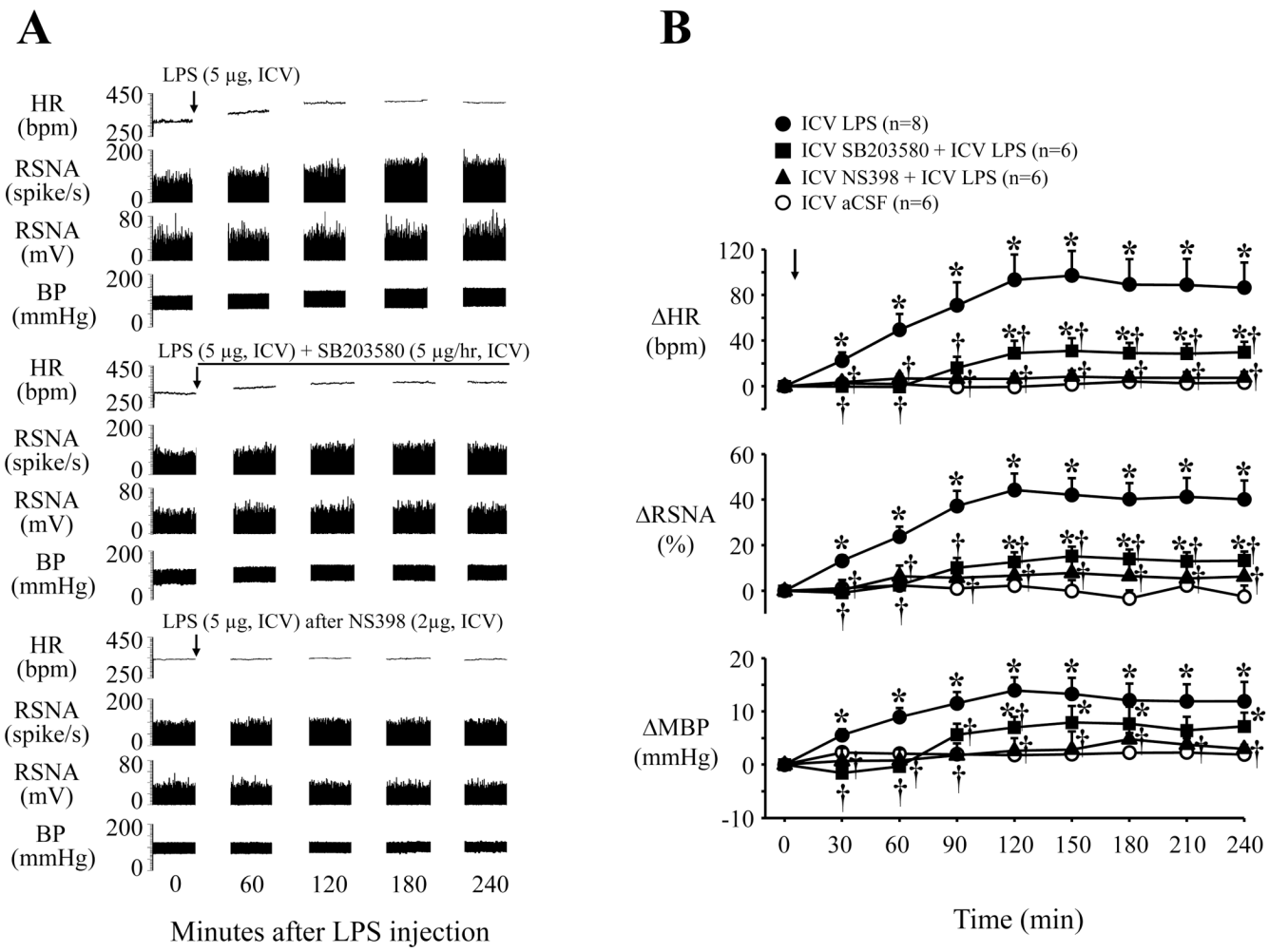

Fig. 5.

Representative recordings (**A**) and grouped data (**B**) showing that central LPS induced sympatho-excitatory responses (increases in HR, RSNA and BP or MBP) can be diminished by continuous ICV infusion of the specific p38 MAPK inhibitor SB203580, and prevented by pretreatment with the specific COX-2 inhibitor NS398. Arrows indicate the ICV LPS injection. Line represents the continuous ICV infusion of SB203580. Each recording section is 200 seconds in duration at 60 min intervals. Values were expressed as mean ± SE. **P*<0.05 versus ICV aCSF, †*P*<0.05, ICV Treatment + ICV LPS versus ICV LPS alone.

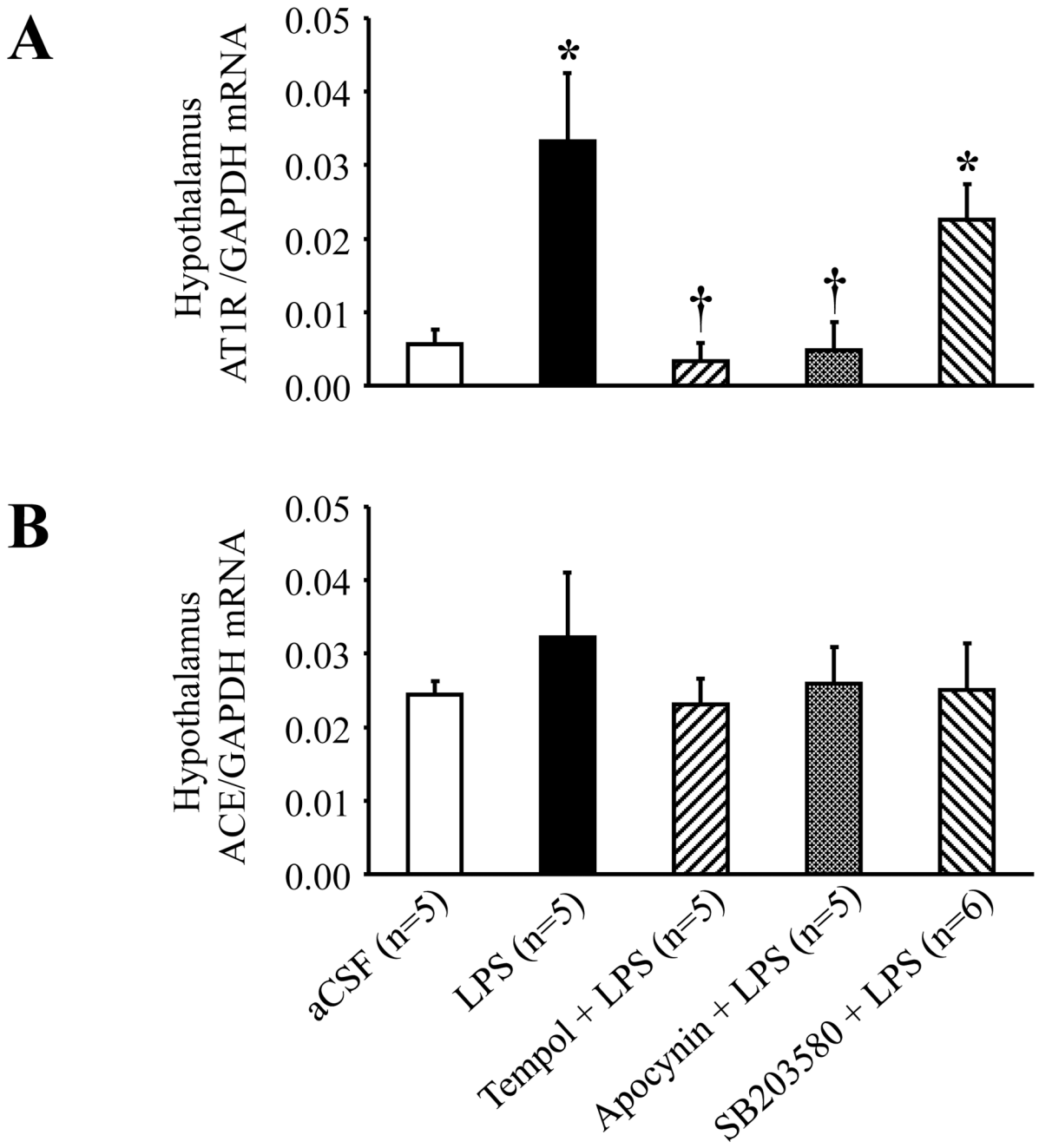

Fig. 6.

Real-time PCR analysis showing increased hypothalamic tissue AT1R (**A**), but not ACE (**B**) mRNA expression 4 hours after ICV administration of LPS. The LPS-induced increase of AT1R mRNA expression was significantly diminished by continuous ICV infusion of tempol and apocynin, but not by SB203580. **P*<0.05 versus ICV aCSF; †*P*<0.05, ICV Treatment + ICV LPS versus ICV LPS alone.

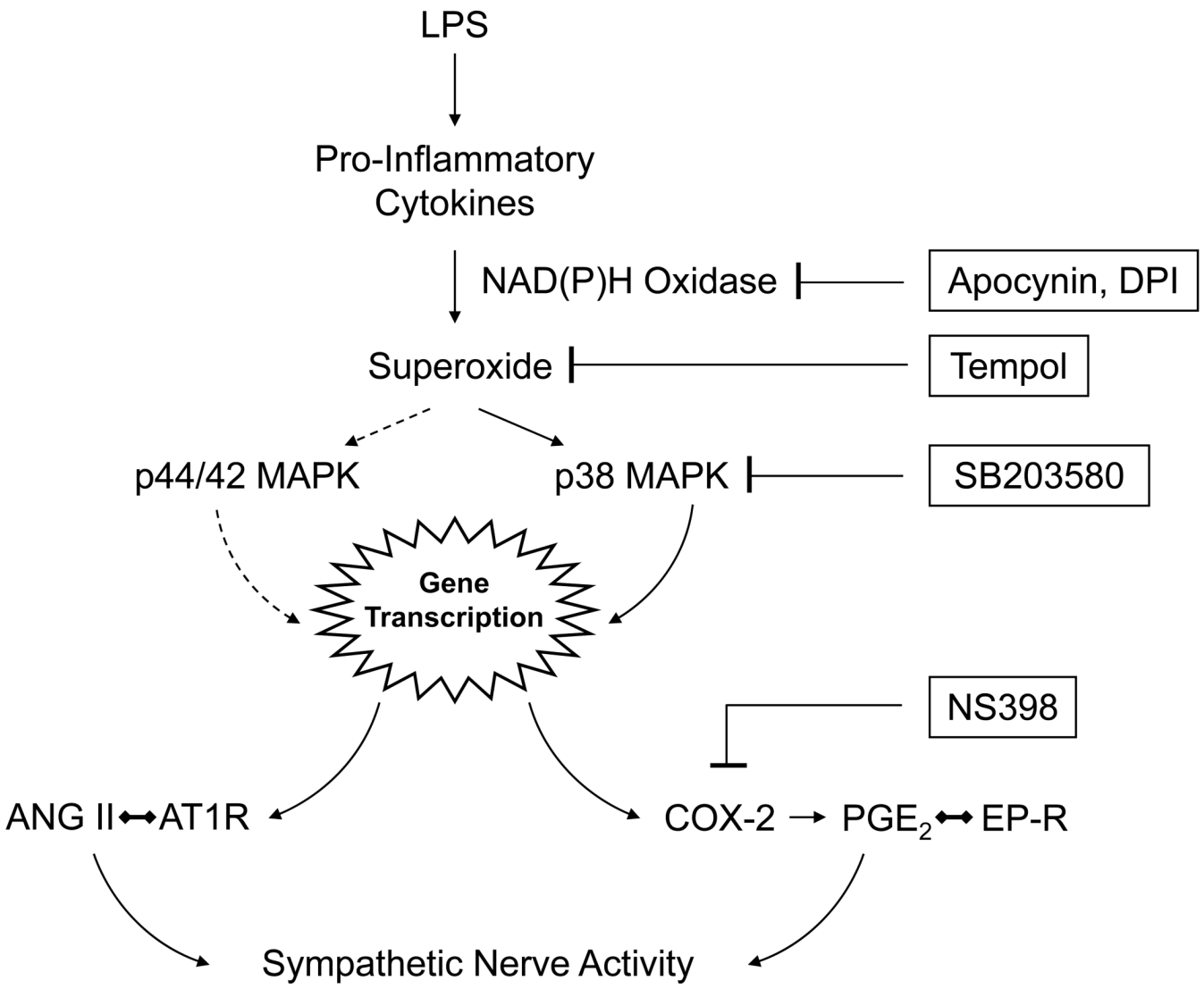

Fig. 7.

Schematic illustrating putative molecular pathways mediating the effects of centrally administered LPS on sympathetic drive. LPS induces the production of pro-inflammatory cytokines, such as TNF-α, with subsequent induction of NAD(P)H oxidase dependent superoxide production. LPS also induces p38 MAPK, which is redox dependent. Downstream gene products of p38 MAPK include COX-2, the enzyme that generates PGE2. PGE2 activates E class prostanoid receptors (EP-R) to activate the sympathetic nervous system. LPS also induces expression of mRNA for the angiotensin II type 1 receptor (AT1R). The LPS induced sympatho-excitatory response can be blocked by inhibiting the LPS-induced NAD(P)H dependent p38 MAPK pathway with blockers or inhibitors at the levels indicated (see text for details). The increase in AT1R mRNA is blocked by agents that reduce superoxide production, but not by the p38 MAPK inhibitor, suggesting an alternative mechanism for that effect. LPS activation of the p44/42 MAPK pathway, which is also redox dependent, might account for this effect.

Table 1

Sequences for primers and probes

Gene	Primers and Probes
COX-2	forward primer: 5’-CGCTGTACAAGCAGTGGCAAAG-3’
	reverse primer: 5’-GCGTTTGCGGTACTCATTGAGA-3’
	probe: 5’-CCTCCATTGACCAGAGCAGAGAGATGAAA-3’
TNF-α	forward primer: 5'-CCAGGAGAAAGTCAGCCTCCT-3'
	reverse primer: 5'-TCATACCAGGGCTTGAGCTCA-3'
	probe: 5'-AGAGCCCTTGCCCTAAGGACACCCCT-3'
p47*phox*	forward primer: 5'-ACGCTCACCGAGTACTTCAACA-3'
	reverse primer: 5'-TCATCGGGCCGCACTTT-3'
	probe: 5'-CCCGCTGCCCACACCTCTTGAACT-3'
gp91*phox*	forward primer: 5'-AAAGGAGTGCCCAGTACCAAAGT-3'
	reverse primer: 5'-TACAGGAACATGGGACCCACTAT-3'
	probe: 5'-CCGGAAACCCTCCTATGACTTGGAAATG-3'

COX-2, cyclooxygenase-2; p47 phox and gp91phox, NAD(P)H oxidase subunits; TNF-α, tumor necrosis factor-alpha.